Real-time modulation of Si-H vibration in hydrogenated amorphous silicon

Hidetoshi Oheda
Electrotechnical Laboratory, 1-1-4 Umezono, Tsukuba, Ibaraki 305-8568, Japan
(Received 20 April 1998; revised manuscript received 27 May 1999)

Photomodulation of Si-H stretching vibration can be observed in hydrogenated amorphous silicon (a-S:H) as a photoinduced bleaching (PB) band around 2000 cm^{-1} which is embedded in a photoinduced absorption spectrum coming from excess carriers trapped at tail states. Since this vibronic modulation is a real-time change following a modulated excitation, it is different from a well known metastability in a-Si:H as induced by strong light soaking. It is suggested from the theoretical work reported by Yonezawa *et al.* [J. Non-Cryst. Solids **137&138**, 135 (1991)] that the modulation of a Si-H vibration reflects a change in length of a neighboring weak Si-Si bond following a modulated excitation. Based on this picture, we have tried to see how the spectrum of the PB band changes when the weak Si-Si bonds are broken or reformed by light soaking or thermal annealing, respectively. Change in the spectrum after the treatments could be observed over almost a whole range of the PB band and this vibronic modulation seems to be related selectively with the monohydride configuration of Si-H bond. By evaluating quantitatively the spectral change in the PB band combined with simultaneous change in dangling-bond density, density of the weak Si-Si bonds or neighboring Si-H bonds responsible for the vibronic PB band can be estimated to be about 5×10^{17} cm^{-3}. This value is much smaller than the amount of the monohydride Si-H bonds contained in specimens used here by about four orders of magnitude, indicating that only a very small part of the existing Si-H bonds participates in the structural flexibility in a-Si:H. [S0163-1829(99)05647-7]

I. INTRODUCTION

Since amorphous materials take disordered structural configuration, they are energetically not in thermal equilibrium in contrast with crystalline materials. It causes a characteristic feature of structural flexibility or metastability in amorphous materials such as photostructural changes observed in chalcogenide glasses or light-induced defect-creation in hydrogenated amorphous silicon (a-Si-H).[1] The latter phenomenon is known as the Steabler-Wronski effect (SW effect) and leads to degradation of quality of various kinds of properties in a-Si:H, including light-induced changes of infrared (IR) absorption spectrum related to Si-H vibrations.[2–4] The SW effect has attracted great interest and many models have been proposed, since the effect is just related to fundamental characteristics of the metastability in the amorphous materials. One plausible model given earlier is that recombination between photogenerated electrons and holes promotes breaking of weak Si-Si bonds with an aid of local H motion to stabilize induced dangling bonds.[5,6] But a recent electron-spin-resonance (ESR) hyperfine study[7] has presented an evidence which does not reconcile with this model: the light-induced dangling bonds did not exhibit spatial correlation with H atoms. In order to overcome this discrepancy with the experimental result, Branz has proposed recently an alternative possibility as the hydrogen collision model,[8] in which he has devised to involve long-range diffusion of mobile H. In his model, creation of the light-induced dangling bonds is assumed to be initiated by producing a mobile H after breaking a Si-H bond. So it is considered that excess energies released by the recombination between excited carriers are dissipated by breaking Si-H bonds instead of weak Si-Si bonds. Anyway, in the SW effect, a photodegraded state is stable as far as the material is held at room temperature.

In contrast with such a light-induced metastable change, Vardeny *et al.*[9] found another kind of light-induced structural change, i.e., real-time modulation of a local structural unit. They observed a dip around 2000 cm^{-1} in a photoinduced absorption (PA) spectrum of a-Si:H when the PA spectrum was measured at an IR region down to around 0.1 eV. It is well known that the PA spectrum at such a near IR region is related mainly with excess carriers trapped at tail states;[9,10] optical absorption between tail states and a nearby extended state is enhanced under illumination. Whereas the dip signal has an opposite sign with respect to the background PA signal, since it appears as the dip band in the spectrum, optical absorption related with the dip band is reduced under illumination.[9] It can be said that the dip is a photoinduced bleaching (PB) band. Vardeny *et al.*[9] speculated that the PB band came from modulation of Si-H stretching vibration following a modulated excitation, since the peak position and width of the PB band coincided well with those of IR absorption of the Si-H stretching vibration at 2000 cm^{-1}. It means that some nature of a Si-H oscillator should vary with time following the modulated excitation. It should be noticed that the vibronic modulation is observable against a band gap excitation whose intensity is low enough not to induce the SW effect.

Since it is hard to consider that a band gap light affects the vibronic mode directly, the modulation of the Si-H vibration will be induced by some structural change around the Si-H bond. Hirabayashi *et al.*[11] pointed out a possibility that the Si-Si bond next to the Si-H bond is weak owing to a difference in electronegativities between Si and H atoms. Subsequently, Yonezawa *et al.*[12] have demonstrated by simulation that length of the weak Si-Si bond neighboring the Si-H bond enlarges under illumination: the length of the weak Si-Si bond is expected to vary with time as if

TABLE I. Characteristics of specimens. T_S, d, and N_D are the substrate temperature during deposition, the film thickness, and the defect density, respectively. N_D for specimen A is the value after annealing at 200 °C and those for specimens B, and C are the values in the as-deposited state. The last three columns summarize hydrogen contents of 2000 and 2100 cm^{-1} modes as well as the total contents.

Specimen	T_S (°C)	d (μm)	N_D (cm^{-3})	2000 cm^{-1} mode (cm^{-3})	2100 cm^{-1} mode (cm^{-3})	Total H (cm^{-3})
A	300	6.3	4.0×10^{15}	4.6×10^{21}	1.3×10^{21}	5.9×10^{21} (10.6 at. %)
B	50	3.7	2.8×10^{18}	3.3×10^{21}	1.3×10^{22}	1.6×10^{22} (24.1 at. %)
C	100	5.0	1.5×10^{18}	3.6×10^{21}	8.5×10^{21}	1.2×10^{22} (19.5 at. %)

breathing following the periodically modulated excitation. As suggested by those works, it is probable that the vibronic PB band reflects a real-time change in the length of the weak Si-Si bond next to the Si-H bond following the modulated excitation. The local structural change around the weak Si-Si bond will take place without breaking any bond in contrast with the situations as assumed in the models[5,6,8] for the SW effect.

If such a syncronized change in the length of the weak Si-Si bonds actually takes place under the modulated excitation, the photomodulation of the Si-H vibration, which gives rise to the PB band, will cease when the neighboring weak Si-Si bond is broken, and a close correlation is expected to exist between changes in the vibronic PB spectrum and dangling-bond density. Base on this idea, we have studied how the PB spectrum is affected when the weak Si-Si bonds are broken or reformed intentionally.

Before presenting experimental results, influence of interference effects in thin films on transmittance change in a modulation spectroscopy will be discussed in Sec. III.

II. EXPERIMENT

In order to modify density of the weak Si-Si bonds, two kinds of treatments were made: strong light soaking for breaking the weak Si-Si bonds and thermal annealing for reforming the broken bonds. Three a-Si:H films were used in the present work. They were deposited on intrinsic crystalline silicon wafers by rf plasma-assisted chemical vapor deposition. The substrate temperature during the deposition, the film thickness, and the defect density for each specimen are summarized in Table I. The specimen A, which was used for the light-soaking study, had a good quality in the as-deposited state. The specimens B and C were very defective in the as-deposited state and were used for the thermal annealing study. Hydrogens included in a-Si:H network take two different bonding configurations of Si-H and Si-H_2. The amounts of hydrogens contributing to respective bonding configurations were evaluated from IR absorption spectrum of the Si-H stretching vibrations by deconvoluting it into 2000 and 2100 cm^{-1} components and by using the conversion factors derived by Langford *et al.*[13] Results are also listed in Table I.

In order to detect spectral change of the modulated IR absorption of the Si-H vibrations after the treatments, a photomodulation (PM) spectrum was measured at the IR region especially around 2000 cm^{-1}. An optical setup for the measurement was almost the same as that used for conventional PA measurement.[10] A specimen which was held within a cryostat was excited with a modulated pump light and induced transmittance change was monitored with a probe light. As the pump light, the 1.83 eV or 1.92 eV line from a Kr^+ laser was used with modulating at 30 Hz. A light from an IR light source was used as the probe light and was focused with an ellipsoidal mirror onto the same area of the specimen where the pump light was illuminated. After passing through the specimen, the probe light was collimated into a liquid-nitrogen cooled HgCdTe detector after dispersed with a monochrometor with a 25 cm focal length combined with a filter. Transmittance T and its modulated change ΔT were measured separately. After that, a ratio between ΔT and T was plotted as a PM spectrum. In the measurement, a slit width of the monochrometor was fixed at 2 mm: a spectral resolution was 16 cm^{-1} at around 2000 cm^{-1}. Dangling-bond density was evaluated with an electron-spin-resonance (ESR) spectrometer; this measurement was possible only at room temperature.

In the study on a light-soaking effect, the specimen A was annealed at 200 °C in vacuum for 5 h before performing every light soaking. The dangling-bond density in the annealed state was evaluated before installing the specimen within the cryostat. After that, the PM spectrum in the annealed state was measured at 13 K. Since the 1.92 eV line had the strongest power among available lines from the Kr^+ laser, it was used as a source for the light soaking as well as the pump light in the PM measurement. An intensity of the 1.92 eV line was 2.1 mW cm^{-2} when it was used as the pump light, whereas it was enhanced up to 2 W cm^{-2} during the light soaking. The light soaking was made at room temperature by holding the specimen within the cryostat after completing the measurements in the annealed state. After the light soaking, the PM spectrum was measured first at 13 K. Then ESR spin density was evaluated again at room temperature.

The other study on a thermal-annealing effect was made with the specimens B and C. Thermal annealing was made at several temperatures between 100 and 230 °C for 3 h in vacuum with taking the specimen out of the cryostat. At each thermal annealing step, ESR spin density was evaluated first at room temperature and, subsequently, the PM spectrum was measured at 13 K. In this study, the 1.83 eV line of the

Kr^+ laser with an intensity of 17 mW cm^{-2} was used as the pump light in the PM measurement.

III. INFLUENCE OF INTERFERENCE ON $\Delta T/T$

When a thin film of solid is illuminated with a modulated excitation, a spectrum of ΔT exhibits interference fringes. Since ΔT depends on a change in complex dielectric constant, $\Delta T/T$ itself does not give any physical meaning. In this section, we examine by simulation how each of the changes in absorption coefficient and refractive index ($\Delta\alpha$ and Δn, respectively) contribute to $\Delta T/T$ at the IR region focused here.

We will consider that a system consists of a thin *a*-Si:H absorbing layer (medium 1) on a semi-infinite crystalline substrate (medium 2). An expression for the transmittance of the thin film is obtained by taking into account the multiple reflections of coherent light inside the film. In the case of normal incidence, it is given by the following equations:[14]

$$T=(1+\kappa^2/n^2)(1-R_{01})(1-R_{21}) \times\exp(-\alpha d)[1-2(R_{01}R_{21})^{1/2}\exp(-\alpha d) \times\cos(2kd+\phi_{01}+\phi_{21})+R_{01}R_{21}\exp(-2\alpha d)]^{-1}. \tag{1}$$

$\kappa=\alpha\lambda/4\pi$ is the extinction coefficient and $k=2\pi n/\lambda$ the wave vector (λ is the vacuum wavelength), where α and n are the absorption coefficient and refractive index of the film (medium 1), respectively. Here, n and κ are the real and imaginary parts of the complex dielectric constant, respectively. R_{01} and R_{21} are the reflectivities of the vacuum-film and film-substrate interface, respectively,

$$R_{i1}=[(n_i-n)^2+\kappa^2]/[(n_i+n)^2+\kappa^2], \tag{2}$$

with i referring either to vacuum (0) or the substrate (2). ϕ_{01} and ϕ_{21} are phase shifts due to the absorption coefficient of the film and are expressed as

$$\phi_{i1}=\arctan[2n_i\kappa/(n^2+\kappa^2-n_i^2)]. \tag{3}$$

According to Eqs. (1)–(3), we can calculate spectral dependences of T, $\partial T/\partial\kappa$, and $\partial T/\partial n$. In the calculation, it is assumed that $n=3.6$ (a typical value for *a*-Si:H), $n_0=1$, $n_2=3.42$ (the value for crystalline Si), and $d=6.3\,\mu$m. The simulation is made at the IR region below 5000 cm^{-1} where $\kappa\ll 1$. Then κ can be neglected in R_{01} and R_{21}, and ϕ_{01} and ϕ_{21} can be also set to zero, although $\partial\phi_{01}/\partial\kappa$ and $\partial\phi_{21}/\partial\kappa$ are not negligible. Figure 1 shows the calculated spectrum of T. Because of the small difference in the refractive indexes between the film and substrate, interference fringes appear very weakly.

By expanding the right-hand side of Eq. (1) in terms of κ and n to the first order, the following relation is obtained:

$$\Delta T=(\partial T/\partial\kappa)\Delta\kappa+(\partial T/\partial n)\Delta n. \tag{4}$$

This relation can be expressed alternatively by changing the variable from κ to α:

$$\Delta T=(\partial T/\partial\alpha)\Delta\alpha+(\partial T/\partial n)\Delta n. \tag{4'}$$

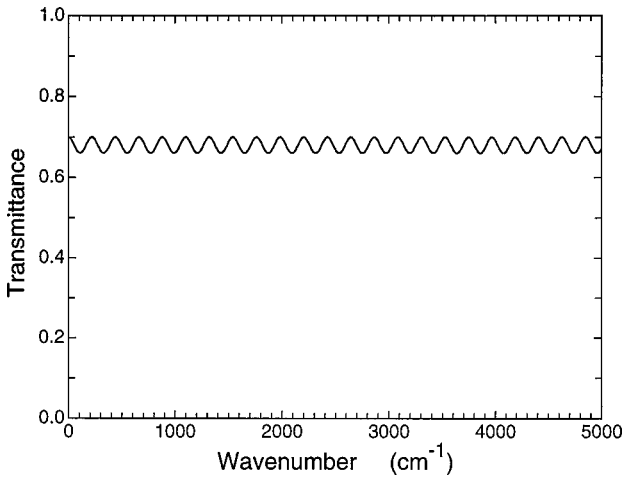

FIG. 1. Simulated transmittance spectrum, which is calculated according to Eq. (1) for $n=3.6$, $n_0=1$, $n_2=3.42$, and $d=6.3\,\mu$m.

Then the quantity of $\Delta T/T$, which will be discussed in the following, can be written formally as

$$\Delta T/T=f_\alpha\Delta\alpha d+f_n\Delta n, \tag{5}$$

where the coefficients f_α and f_n are expressed respectively as

$$f_\alpha=(1/T)(1/d)(\partial T/\partial\alpha)=(1/T)(\lambda/4\pi d)(\partial T/\partial\kappa) \tag{6}$$

and

$$f_n=(1/T)(\partial T/\partial n). \tag{7}$$

The analytical expressions for f_α and f_n can be derived from Eqs. (1)–(3), based on which spectral dependences of f_α and f_n are calculated by using the same values for n, n_0, n_2, and d as in Fig. 1. Figures 2(a) and 2(b) are the calculated spectra of f_α and f_n, respectively, at wave numbers below 5000 cm^{-1}. As one can see from the figures, both quantities are affected by the interference effect. However, there is some qualitative difference between f_α and f_n. The interference fringes in the f_α spectrum do not change their sign and oscillate around -1. The oscillating amplitude is small as compared to the mean value of -1 and keeps an almost constant value of 0.03 above 1000 cm^{-1}. In contrast to f_α, the oscillating amplitude of f_n increases gradually with wave number and its sign changes preriodically. These qualitative differences help to distinguish whether induced absorption or induced refractive index changes make the dominant contribution to $\Delta T/T$: presence or absence of sign changes in the $\Delta T/T$ spectrum can be used to judge when it exists.[15]

A typical PM spectrum for the specimen *A* with the thickness of 6.3 μm after annealing at 200 °C is shown with dots in Fig. 3, in which a simulated spectrum fitted to the measured spectrum is shown with a thin solid line. The oscillating part of the measured spectrum can be fitted well with a sine wave having an amplitude which holds a constant ratio with respect to a mean value of $\Delta T/T$ at any wave number. If the second term in Eq. (5) is not negligible, the oscillating amplitude should grow with wave number more enhancedly, since not only f_n but also the mean value of $\Delta T/T$ increase with the wave number. But the oscillating part of the spectrum in Fig. 3 can be fitted by the sine wave having a con-

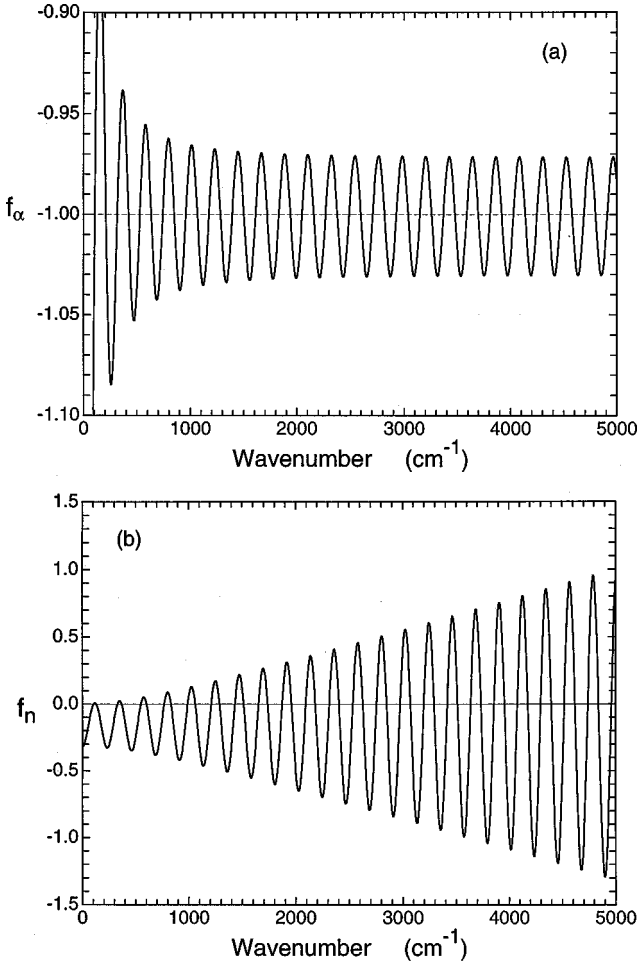

FIG. 2. Coefficients in Eq. (5) as a function of wave number; (a) for f_α and (b) for f_n. They are calculated by using the same values as in Fig. 1.

stant relative amplitude and, furthermore, any evidence of the sign change cannot be seen in the spectrum. So that a contribution to $\Delta T/T$ from the change in the refractive index is negligible for the present case at the IR region studied here. As a result, $\Delta T/T$ can be regarded as

$$\Delta T/T \approx f_\alpha d\Delta\alpha(\lambda), \tag{8}$$

where $\Delta\alpha(\lambda)$ represents the absorption coefficient when it generally depends on λ.

$\Delta T/T$ in Fig. 3 took a negative value within the measured energy range, indicating that optical absorption of the specimen was enhanced under illumination of the pump light as usually observed.[9,10] Embedded in this overwhelming background PA spectrum, a dip can be noticed around 2000 cm^{-1} in spite of the presence of interference fringes.

IV. RESULTS

Dots in the lower figure of Fig. 4 shows an expanded PM spectrum around 2000 cm^{-1} for the specimen *A*. A structure observed around 2300–2400 cm^{-1} in the spectrum might be induced by unexpected fluctuations of absorption of CO_2 in air during the alternate measurements of ΔT and T. For the sake of separating a pure PB band from a measured PM spectrum, we have simulated a background PA spectrum ex-

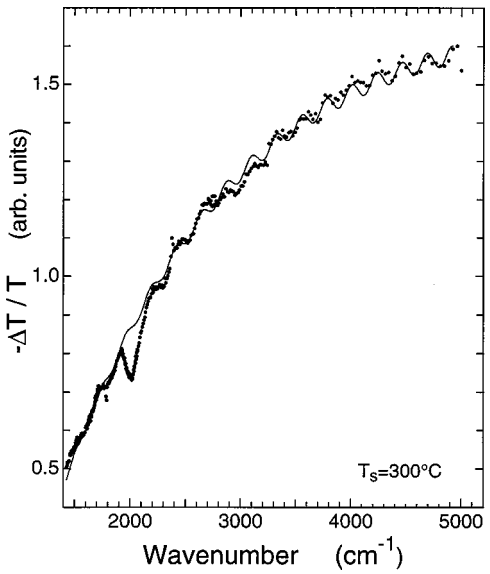

FIG. 3. A typical photomodulation spectrum for the specimen A. A simulated spectrum fitted to the measured spectrum is shown with a thin solid line. Observed interference fringes can be fitted well with a sine wave having an amplitude which holds a constant ratio with respect to a mean value of the spectrum at any wave number. In spite of the presence of interference fringes, a dip is noticeable around 2000 cm^{-1}.

cept a dip band. Following the arguement in the previous section, simulation of the background PA spectrum can made based on Eq. (8). The right-hand side of this equation is a product between f_α and $d\Delta\alpha(\lambda)$. When relating them to an

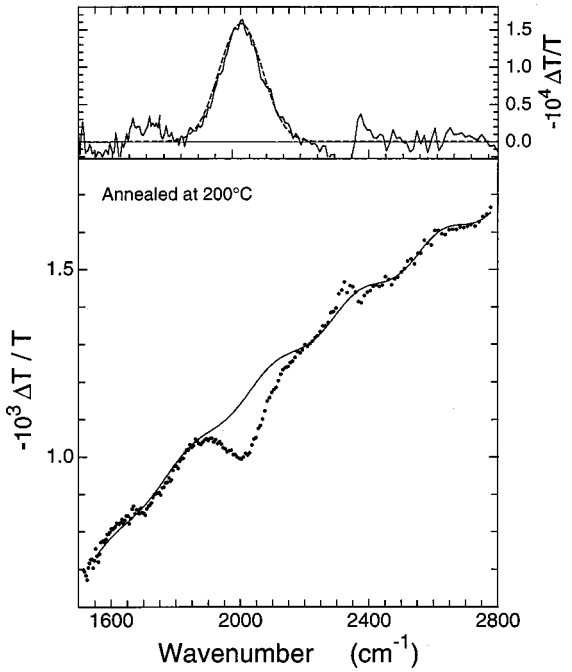

FIG. 4. The lower figure shows a photomodulation spectrum for the specimen A after annealing at 200 °C for 5 h: dots represent raw data and a solid line is the simulated background PA spectrum. The pure PB spectrum can be separated from the measured PM spectrum by subtracting the simulated PA spectrum, and is shown above in the figure. The separated pure PB spectrum can be fitted with a single Gaussian line (a broken line).

observed PA spectrum, $d\Delta\alpha(\lambda)$ corresponds to an averaged PA spectrum and a contribution of the interference fringes is included in f_α. Since f_α keeps an almost constant value above 1000 cm^{-1} as demonstrated in Fig. 2(a), f_α is expressed approximately by $-1+m\sin(D/\lambda+\phi)$, where D is a constant, which depends on d, ϕ is a term related with optical phase shifts, and m is a modulation depth. Combining with a simulation of the averaged PA spectrum using an adequate polynomial, the oscillating part of the spectrum could be simulated successfully by adjusting the independent variables of D, ϕ, and m in the approximate expression for f_α. When a film was thick enough as the specimen *A*, the fitting could be made with good accuracy. Even when a film became slightly thinner as the specimen *B* or *C* with more elongated periodicity of the interference fringes, its wavy background spectrum could be simulated well as shown later in Fig. 10.

Thus simulated background PA spectrum for the specimen *A* is shown with a solid line in the lower figure in Fig. 4. By subtracting the simulated PA spectrum from the measured PM spectrum, the pure PB spectrum can be obtained. The upper figure in Fig. 4 shows thus obtained pure PB spectrum in the annealed state, which can be fitted with a Gaussian line (a broken line) which is centered at 2025 cm^{-1} and has the full width at half maximum (FWHM) of about 150 cm^{-1}. As pointed out in the Introduction, those values correspond well to the characteristics of the IR-absorption spectrum of the Si-H stretching mode in the specimen *A*. Roughly speaking, magnitude of the PB band is smaller than that of the PA signal around 2000 cm^{-1} by about an order. Since the background PA spectrum itself is likely to be altered through the light soaking or thermal annealing, simulation of the background PA spectrum was made for each case when necessary.

A. Effect of light soaking

Figure 5(a) shows the PM spectra for the specimen *A* in the annealed and subsequent light-soaked states when the light soaking was made at room temperature. We have measured only a limited part of the PM spectrum around 2000 cm^{-1} with great care. Magnitude of the PM spectrum was reduced succesively with increasing light-soaking time. However, 24 h of light soaking was almost sufficient to reach saturation at room temperature. Reproducibility of the PM spectra in Fig. 5(a) was confirmed by repeating several times the measurements between the annnealed and 24 h light-soaked states. Such a change of the PM spectrum through photodegradation was observed more enhancedly when the light soaking was made at 13 K as shown in Fig. 5(b). The amount of change in the PM signal induced by the 20 h light soaking at 13 K was larger than that induced by the 24 h light soaking at room temperature by a factor of 1.34. It seems that there exists a difference in nature of the light-soaked state depending on at which temperature the light soaking is made. When the light soaking was made at room temperature, the light-soaked state was stable as far as holding the specimen there, whereas partial recovery of the PM spectrum could be observed when the specimen was warmed up to room temperature after the light soaking at 13 K. In Fig. 5(b), the spectrum labeled ''Recovered'' is the one measured after holding the specimen at room temperature for 2 days after the light soaking at 13 K. The partially recovered spectrum took almost the same magnitude as the spectrum in the state light soaked at room temperature for 24 h. The recovery of the PM spectrum as shown in Fig. 5(b) indicates that some part of the light-induced change is stable only at a low temperature. This phenomenon is not discussed any more since later analysis will be concerned mainly with the results in Fig. 5(a).

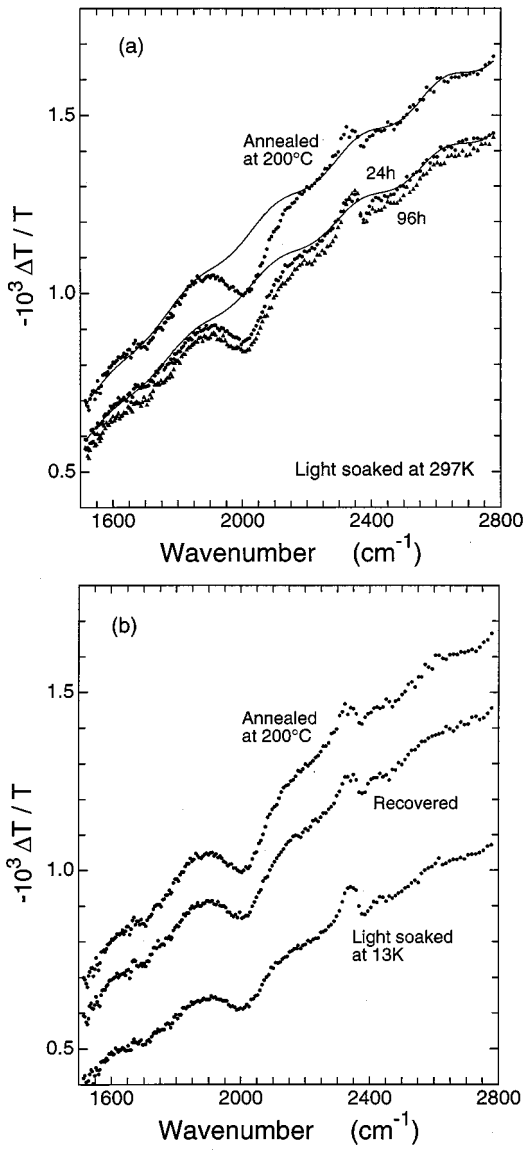

FIG. 5. Photomodulation spectra for the specimen A in the annealed and subsequent light-soaked states; (a) and (b) summarize results for the light soaking at 297 K for 24 and 96 h and 13 K for 20 h, respectively. Dots represent raw data and solid lines in (a) are the simulated background PA spectra. The spectrum labeled ''Recovered'' in (b) is measured after holding the specimen at room temperature for 2 days after the light soaking at 13 K.

The background PA spectra for the state light soaked at 297 K for 24 h as well as that for the annealed state are simulated as demonstrated with solid lines in Fig. 5(a). A comparison between the separated pure PB spectra before and after the light soaking is made in the lower figure of Fig. 6. Difference spectrum is shown in the upper figure. It can be

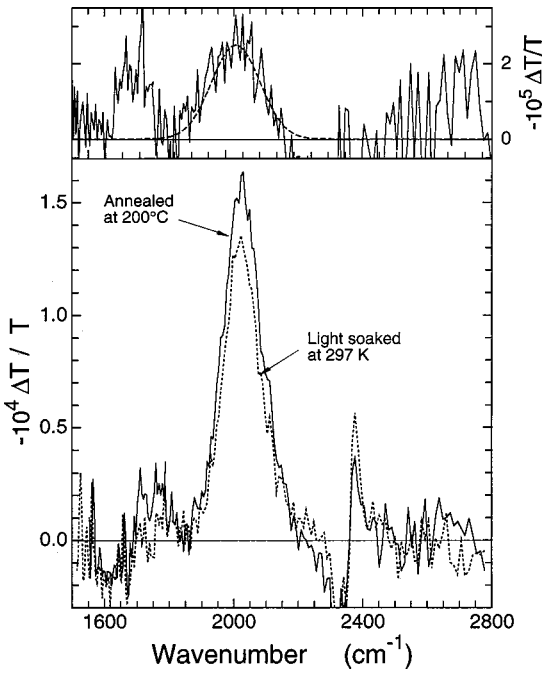

FIG. 6. The lower figure shows a comparison between PB spectrum for the specimen A in the annealed state and that for the state light soaked at 297 K for 24 h. Difference spectrum is shown in the upper figure. It can be fitted with a Gaussian line as shown with a broken line.

fitted with a single Gaussian line (a broken line) which is centered at 2030 cm^{-1} and has the FWHM of about 150 cm^{-1}, indicating that the spectral change took place almost uniformly over the whole range of the PB band. An additional structure observed around 1700 cm^{-1} in the difference spectrum may be an artifact due to incompleteness in fitting the PA spectrum. Although a result is not shown here, change in the PB spectrum was induced more enhancedly by about a factor of 2 when the light soaking was made at 13 K.

B. Effect of thermal annealing

We have made a complementary study with the specimens *B* and *C* about how the PB spectrum is modified through structural relaxation induced by the thermal annealing. In the as-deposited state, the PM signals were not detectable for the specimen *B* or were very noisy for the specimen *C* at the IR region focused here. So the states annealed at 100 °C for 1 h and at 120 °C for 3 h were chosen here as the starting state for specimens *B* and *C*, respectively. Subsequent thermal annealings were made at several temperatures up to 230 °C. With increasing annealing temperature, the magnitude of the PM signal was recovered gradually and the ESR spin density was reduced on the contrary. Since a way of changing those quantities during the thermal annealing was almost the same in both specimens, results and their analysis were detailed below mainly for the specimen *B*.

Summarized results for the specimen *B* are shown in Figs. 7 and 8 for $\Delta T/T$ at 2000 cm^{-1} and the ESR spin density, respectively. The values of both quantities were almost saturated after annealing at 230 °C. Figure 9 shows the PM spectra at some representative annealing temperatures. Although a more intense probe light was used in this study as compared with the light-soaking study in the previous section, the absolute magnitude of $\Delta T/T$ for the specimen *B* even after annealing at 230 °C was much smaller than that for the specimen *A* after the 24 h light soaking at room temperature.

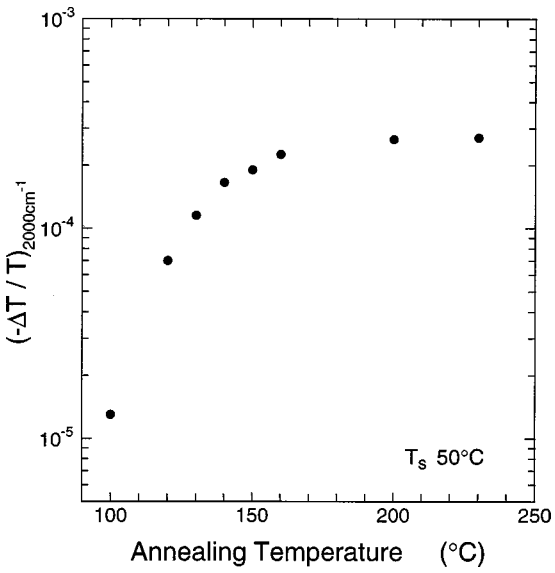

FIG. 7. Recovery of photomodulation signal at 2000 cm^{-1} for the specimen B with increasing annealing temperature.

The PM spectrum after annealing at 230 °C is shown in the lower figure of Fig. 10(a), in which a solid line represents the simulated background PA spectrum. The separated pure PB spectrum is shown in the upper figure and can be fitted well with two Gaussian lines (broken lines) peaked at 2050 and 2230 cm^{-1} with the common FWHM of 200 cm^{-1}. Interestingly, the component nearby 2000 cm^{-1} is stronger than the other, although the IR absorption of the Si-H stretching vibration for the specimen *B* is dominated mainly by the 2100 cm^{-1} mode. In the following analysis, the PB spectrum measured after annealing at 230 °C is regarded as the one in the well annealed state.

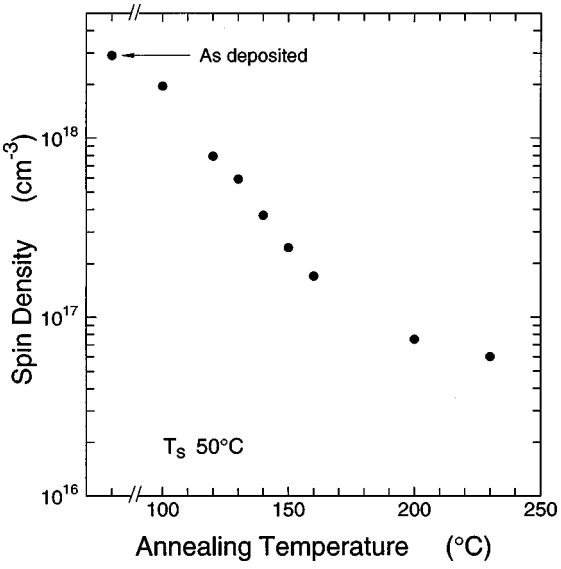

FIG. 8. Decrease in ESR spin density for the specimen B with increasing annealing temperature.

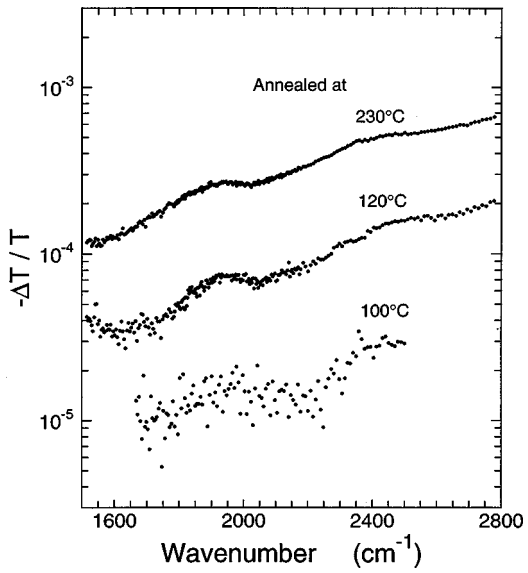

FIG. 9. Evolution of photomodulation spectra for the specimen B with increasing annealing temperature.

The PM spectrum after annealing at 120 °C is shown in the lower figure of Fig. 10(b), in which a solid line represents the simulated background PA spectrum, too. In this case, the separated pure PB spectrum shown in the upper figure of Fig. 10(b) can be also fitted with two Gaussian lines (broken lines) peaked at the same wave numbers as in the 230 °C annealed state. A comparison between the pure PB spectra after annealing at 120 and 230 °C is made in the lower figure of Fig. 11. The difference spectrum is shown above in Fig. 11. It can be fitted with two Gaussian lines (broken lines) peaked at 2040 and 2220 cm^{-1} with the common FWHM of 200 cm^{-1}. Although the difference spectrum ranges relatively wide in the wave number, it is dominated mainly by the component nearby 2000 cm^{-1}.

V. DISCUSSION

A. Density of weak Si-Si bonds responsible for the structural flexibility

As expected before starting this work, the vibronic PB band was actually affected by the light soaking or thermal annealing. From the experimental results, we can evaluate the density of weak Si-Si bonds having a potential to contribute to the vibronic PB band. In each of the light-soaking and thermal annealing studies, the spectral area of the pure PB spectrum in the state with lower defect density is denoted as S_0, and that of the induced change in the PB spectrum after the treatments as ΔS. On the other hand, the density of the weak Si-Si bonds in the well annealed state with lower defect density is denoted as N_0, and the density of the weak Si-Si bonds which are actually broken or reformed through the treatments as $\Delta N/2$, where ΔN is the induced change in the dangling-bond density and a factor 2 comes from the fact that two dangling bonds are formed after breaking a weak Si-Si bond.[16] Since it is supposed that both changes in the PB spectrum and ESR spin density have the same origin, a ratio between $\Delta N/2$ and N_0 should be equal to a ratio between ΔS and S_0. Then N_0 can be expressed as

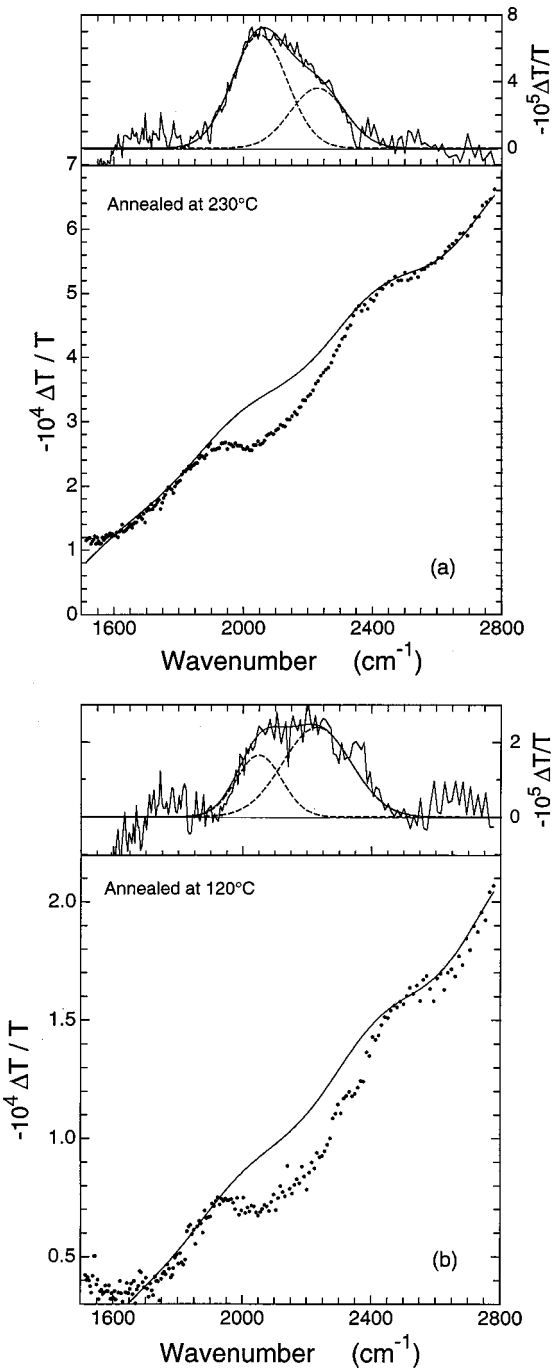

FIG. 10. Dots in the lower figure represent photomodulation spectrum for the specimen B after annealing (a) at 230 °C and (b) at 120 °C. A solid line in the lower figure shows the simulated background PA spectrum. The upper figure shows separated pure PB spectrum, which can be fitted with two Gaussian lines as shown with a broken line (the sum of them is represented with a thin solid line).

$$N_0 = (\Delta N/2) S_0 / \Delta S. \tag{9}$$

In the light-soaking study, S_0 and ΔS are evaluated from the spectral area of the simulated Gaussian curves in Figs. 4 and 6, respectively. In the same way, S_0 and ΔS in the thermal annealing study are evaluated from the spectral area of the simulated curves (each of them consists of two Gaussian curves) in Fig. 10(a) and Fig. 11, respectively. The ratio of

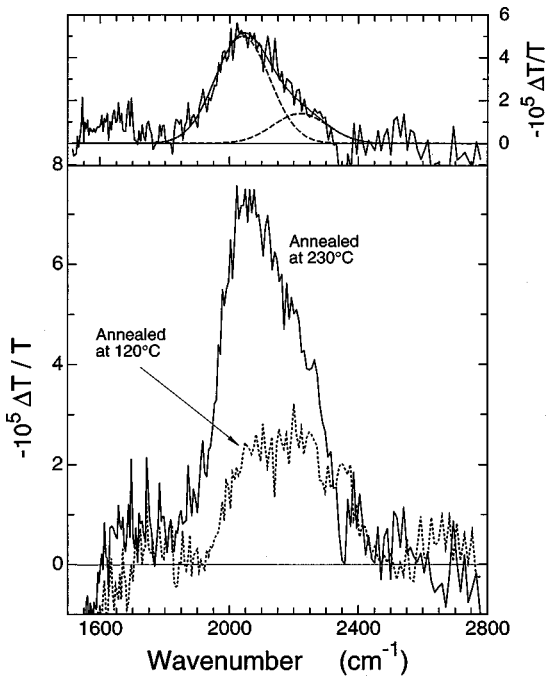

FIG. 11. The lower figure shows a comparison between PB spectra for the specimen B in both states annealed at 120 and 230 °C. The upper figure shows difference spectrum which can be fitted with two Gaussian lines as shown with broken lines (the sum of them is represented with a thin solid line).

$\Delta S/S_0$ as well as the simultaneous change in the dangling-bond density ΔN for each specimen are summarized in Table II.

According to the relation (9), N_0 can be evaluated and the results are listed in Table II as N_0^A: the value of $5.0\times10^{17}\,\mathrm{cm}^{-3}$ is obtained from the light-soaking study and 6.1×10^{17} and $5.5\times10^{17}\,\mathrm{cm}^{-3}$ for the specimens *B* and *C*, respectively, from the thermal annealing study.

B. A relationship between magnitude of the PB band and dangling-bond density

The analysis in the previous section is made based on the assumption that the density of the weak Si-Si bonds responsible for the structural flexibility takes a limited value of N_0: creation or annihilation of the dangling bonds takes place within this limit. When some part of the weak Si-Si bonds is converted to the dangling bonds (their density is ΔN) and the remaining density of the weak Si-Si bonds is ΔN_{Si}, the situation supposed in the previous section can be expressed as

$$(\Delta N/2)+\Delta N_{\mathrm{Si}}=N_0. \tag{10}$$

Furthermore, it is assumed implicitly that ΔN vanishes in the well annealed state. In this limit, the above equation becomes

$$\Delta N_{\mathrm{Si0}}\equiv N_0. \tag{10'}$$

The relation (9) can be derived from Eqs. (10) and (10′) by replacing ΔN_{Si} with a quantity proportional to the magnitude of the PB band.

Now we consider a relationship between the measured quantities of the fractional change in the PB spectrum and of ESR spin density in another way. ΔN is related to the measured ESR spin density N_D by the following relation:

$$N_D=N_{D0}+\Delta N, \tag{11}$$

where N_{D0} represents the density of residual dangling bonds which are free from the exchange interaction with the weak Si-Si bonds. Whereas ΔN_{Si} is related to the magnitude of the PB band, $(-\Delta T/T)_{\mathrm{PB}}$ as argued above. By changing the variables from ΔN and ΔN_{Si} to N_D and $(-\Delta T/T)_{\mathrm{PB}}$, respectively, Eq. (10) can be written alternatively as

$$N_D+c(-\Delta T/T)_{\mathrm{PB}}=2N_0+N_{D0}, \tag{12}$$

where c is a proportionality constant. This gives a direct relationship between N_D and $(-\Delta T/T)_{\mathrm{PB}}$. Figure 12 summarizes results for all specimens. Data for each specimen, except for the point of the starting state for the specimens *B* (the state annealed at 100 °C), can be fitted quite well with a straight line, indicating that, in the course of the light soaking or thermal annealing, the term in the right-hand side of Eq. (12) holds a constant value, which will differ in general depending on the specimens. Then extraporation of the straight line intercepts the N_D axis at $2N_0+N_{D0}$. As can be seen from the figure, extrapolated intercepts at the abcissa for the specimens *B* and *C* locate around $10^{18}\,\mathrm{cm}^{-3}$. Since the residual dangling-bond density N_{D0} in the well annealed state for each specimen was much less than the order of $10^{17}\,\mathrm{cm}^{-3}$, the value at the intercept can be considered to give $2N_0$. Thus evaluated values for N_0 are listed in Table II as N_0^B and coincide well with those evaluated in the previous section. It must be noted that, in the same figure, results for

TABLE II. Density of the weak Si-Si or neighboring Si-H bonds, N_0, which are responsible for the structural flexibility. It is evaluated from the results of light-soaking and thermal annealing studies by two ways. First, N_0 (denoted as N_0^A) is evaluated according to Eq. (9) with values of $\Delta S/S_0$, the relative change of spectral area of the PB spectrum, and of ΔN, the simultaneous change in ESR spin density. Secondly, N_0 (denoted as N_0^B) is evaluated from the results in Fig. 12 according to Eq. (12).

	$\Delta S/S_0$ (%)	ΔN (cm^{-3})	N_0^A (cm^{-3})	N_0^B (cm^{-3})
Light-soaking study (with specimen *A*)	13.9	1.4×10^{17}	5.0×10^{17}	3.5×10^{17}
Thermal annealing study (with specimen *B*)	60.6	7.4×10^{17}	6.1×10^{17}	5.0×10^{17}
Thermal annealing study (with specimen *C*)	44.1	4.9×10^{17}	5.5×10^{17}	4.5×10^{17}

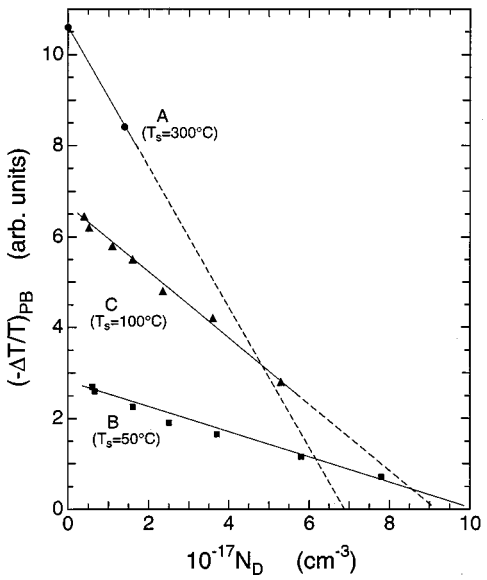

FIG. 12. A relationship between magnitude of the PB band, $(-\Delta T/T)_{\mathrm{PB}}$, and ESR spin density, N_D, for each specimen. Each data set for respective specimens can be fitted with a straight line. Extraporated intersect at the abscissa for each specimen converges around $10^{18}\,\mathrm{cm}^{-3}$.

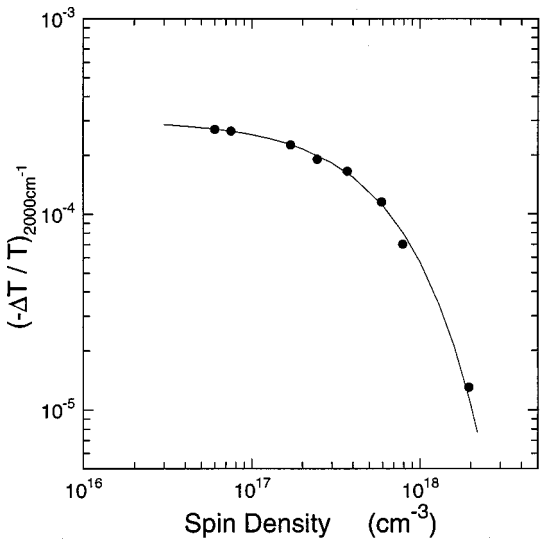

FIG. 13. A relationship between the photomodulation signal at 2000 cm^{-1} and ESR spin density for the specimen B. It is obtained by replotting the results in Figs. 7 and 8.

the specimen *A* are also included. However, since only two points were available, the value for N_0^B for the specimen *A* in Table II, which was evaluated also by extrapolating a straight line through those two points, will not be so accurate. Roughly speaking, N_0 seems to take a common value irrespective of the specimen.

In the above discussions, a defect-quenching effect is not taken into account. However, as you can see in Figs. 5(a), 5(b), and 9, the higher the spin density, the lower the PM signal. Usually, decrease in the magnitude of the PA signal through photodegradation has been considered as a result of enhancement of the defect-quenching effect:[17,18] more and more tail-state carriers are captured by defects when their density is enhanced with proceeding the photodegradation. Figure 13 shows a direct relationship between the PA signal and dangling-bond density for the specimen *B* in a double-logarithmic plot by replotting the results in Figs. 7 and 8. At first sight, it resembles a well known relationship between the photoluminescence (PL) efficiency and defect density. It has been interpreted that decrease in the PL efficiency with the defect density as a result of the defect-quenching effect.[19] So we must look over whether the decrease in the PB signal with N_D as shown in Fig. 13 is affected by the defect-quenching effect.[20]

When the defect quenching is operative, the PB signal after compensating the defect-quenching effect by some means can be expressed as

$$(-\Delta T/T)_{\mathrm{PB}} = Q(N_D)(-\Delta T/T)_{\mathrm{PBM}}, \tag{13}$$

where $(-\Delta T/T)_{\mathrm{PBM}}$ represents the PB signal observed in the measurement and, $Q(N_D)$ is a factor for compensating the defect-quenching effect and depends on N_D. Since $(-\Delta T/T)_{\mathrm{PB}}$ in Eq. (12) represents the PB signal which is free from the effect, the following relation can be derived from Eqs. (12) and (13):

$$(-\Delta T/T)_{\mathrm{PBM}} = [cQ(N_D)]^{-1}(2N_0 + N_{D0} - N_D). \tag{14}$$

Then a derivative of $(-\Delta T/T)_{\mathrm{PBM}}$ with respect to N_D is written as

$$\frac{d(-\Delta T/T)_{\mathrm{PBM}}}{dN_D} = -[cQ(N_D)]^{-1} - \{(2N_0 + N_{D0} - N_D)/[cQ(N_D)^2]\} \times \frac{dQ(N_D)}{dN_D}. \tag{15}$$

This gives a slope of a curve at any N_D when $(-\Delta T/T)_{\mathrm{PBM}}$ is plotted against N_D. Its value will change with N_D through $Q(N_D)$ and $dQ(N_D)/dN_D$ if the defect-quenching effect is operative: for example, even when the second term in the right-hand side of Eq. (15) is negligible, the slope becomes lower and lower with N_D since $Q(N_D)$ is expected to get larger with N_D. But the fact that the relationship between $(-\Delta T/T)_{\mathrm{PBM}}$ and N_D can be fitted with the straight line indicates that, fortunately, it does not need to use the N_D-dependent factor of $Q(N_D)$ or to take into account the defect-quenching effect in the present work. However, the dangling-bond densities in the as-deposited states for the specimens *B* and *C* exceed respective values of N_0^B listed in Table I; if the points in the as-deposited state are plotted in Fig. 12, they will deviate from corresponding straight lines. If more detailed thermal annealing was made at temperatures closer to the substrate temperature of deposition, gradual change in the slope would be observed. The successful fit of the data by the straight line as demonstrated in Fig. 12 certifies the validity of the evaluated values for N_0 (N_0^A and N_0^B in Table II).

C. Structural flexibility in *a*-Si:H

Nearly the same values were evaluated as N_0 irrespective of the specimens. One can find from Table I that the hydrogen contents contributing to the 2000 cm^{-1} component in all

the specimens happen to be almost same, whereas remaining hydrogen contents contributing to the 2100 cm^{-1} component differ by about an order of magnitude among them. So the structural flexibility discussed here is likely to be related especially with the monohydoride mode of the Si-H stretching vibration. This is evidenced by other observation that the spectral change of the PB band for the specimen *B* with a bad quality is also centered nearby 2000 cm^{-1} as demonstrated in Fig. 11, although the 2100 cm^{-1} component is dominant in the IR absorption related with the Si-H stretching vibrations in this specimen. Taking a ratio between N_0 and the amount of the monohydride bonds of Si-H listed in Table I, we can estimate how much fraction of the total weak Si-Si bonds participates in the structural flexibility in each specimen. They are evaluated as 1.1×10^{-4}, 1.9×10^{-4}, and 1.5×10^{-4} for the specimens *A*, *B*, and *C*, respectively. A very small part of the existing weak Si-Si bonds can participate in the structural flexibility, indicating that neighboring to the Si-H bond is not a sufficient condition for selecting a weak Si-Si bond as a source for the structural flexibility.

According to Yoon *et al.*,[21] the defect density induced by a pulsed-light soaking could be reached just below $10^{18}\,cm^{-3}$ at room temperature. This value was commonly established irrespective of the defect density ranging from 3×10^{15} to $5\times10^{16}\,cm^{-3}$ in the annealed state;[21] it seems as if there exists some limited value for the saturated defect density. $2N_0$ evaluated here takes nearly the same value as the saturated defect density established with the pulsed-light soaking. So the weak Si-Si bonds argued in this work may be a good candidate as a source for the saturated defect density, and the modulation of the Si-H vibrational mode should be a phenomenon preceding the photoinduced defect creation.

D. Change in the IR absorption due to S-H vibration after photodegradation and under illumination

When defects are induced by an intense illumination, some structural change is expected to take place locally or within some extended range of space. Until now, many speculations were made about kinetics of the SW effect, but only a few works tried to get a direct evidence for local structural changes. Among several tools for characterizing structural properties of amorphous materials, the IR absorption spectroscopy has been used by several authors to detect a spectral change of the Si-H vibration since hydrogen is considered to participate in the SW effect. However, there exists some controversy among the reported results, especially concerning whether the IR absorption related to the Si-H stretching vibration enhances or not after the photodegradation.

Decrease in magnitude of the IR absorption at 2000 cm^{-1} was reported early by Hong *et al.*[2] Darwich *et al.*[3] reported the same result and, furthermore, they observed a growth of a new band around 1730 cm^{-1} as well as a good correlation between increase in absorption of the bending mode centered at 870 cm^{-1} and decrease in those of the wagging and stretching modes centered at 640 and 2000 cm^{-1}, respectively. Those correlated changes were interpreted by them as suggesting a redistribution of bonded hydrogens in the silicon network through their diffusion during the light soaking.[3] On the other hand, Zhao *et al.*[4] have reported increase in absorption of the 2000 cm^{-1} mode. They have denied a possibility of change in an effective charge of a Si-H dipole and, alternately, interpreted it as a result of creation of additional Si-H bonds. However, the possibility of change in the effective charge of the Si-H dipole was suggested earlier by Oguz *et al.*[22] for interpreting their observed change in the IR absorption after He^+ ion bombardment. Recently, Biswas *et al.*[23] have proposed again the possibility of change in the effective charge by simulation in order to reconsider Zhao's result. They have demonstrated that the dynamic effective charge, the square of which is proportional to the oscillator strength of a dipole,[24] of the Si-H dipole can be enhanced when H is flipped to the backside of Si-H in the normal bonding configuration.[23]

In their simulation study,[23] an interesting result, which is very instructive when considering the present results, has been also presented. Figure 4 in their paper[23] indicates that even the dynamic effective charge of the Si-H bond in the normal bonding configuration will fluctuate depending on a site owing to a difference in local geometry. So it is greatly probable that the IR absorption due to the Si-H bond in the normal bonding configuration will be altered when local geometry around it is modified under illumination. If this is the case, it is supposed that the dynamic effective charge of the Si-H bond in the normal bonding configuration will be reduced under illumination, since the vibronic PB band is a result of decrease in the IR absorption under illumination.

E. Frequency response of the PB signal

In order to get further insight into the vibronic modulation, we will consider how fast the PB signal can follow a modulated excitation. However, it is difficult to measure directly a response time of the pure PB signal, because the PB band is embedded within the intense background electronic PA spectrum. Alternatively, the response time was evaluated

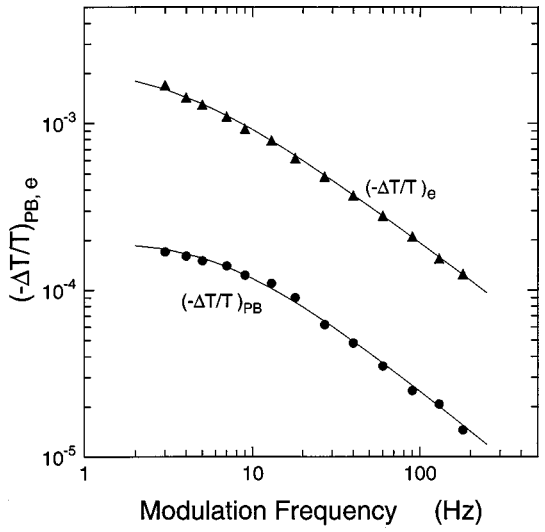

FIG. 14. Modulation-frequency dependences of magnitude of vibronic PB band $(-\Delta T/T)_{PB}$, and of electronic PA signal nearby 2000 cm^{-1}, $(-\Delta T/T)_e$, for the specimen A. They were measured at 13 K using the pump light of the 1.83 eV line with an intensity of 1.1 $mW\,cm^{-2}$.

by measuring a modulation-frequency dependence of the magnitude of the pure PB signal. Here a frequency dependence of $(-\Delta T/T)_{\mathrm{PB}}$, i.e., the absolute magnitude of the pure PB band, was measured at 13 K. When a response time of it is characterized only with a single value, τ_r, $(-\Delta T/T)_{\mathrm{PB}}$ is expected to change with a modulation frequency f as $1/[1+(2\pi f\tau_r)^2]^{1/2}$. Then τ_r can be evaluated by reading a value of the frequency where a break point locates in a double-logarithmic plot between $(-\Delta T/T)_{\mathrm{PB}}$ and f. Figure 14 shows the frequency dependence of $(-\Delta T/T)_{\mathrm{PB}}$ for the specimen *A* which was measured with the pump light of the 1.83 eV line with an intensity of 1.1 mW cm^{-2}. A break point appears around 10 Hz, although it is blurred owing to a distribution of τ_r. The mean response time is evaluated as about 16 ms. In the same figure, the frequency dependence of $(-\Delta T/T)_e$, the magnitude of the electronic PA signal nearby 2000 cm^{-1}, is also shown. A break point in this plot seems to locate at a lower frequency as compared with that of $(-\Delta T/T)_{\mathrm{PB}}$, so that the response time of $(-\Delta T/T)_e$ will be a little longer.

Since the modulation of the Si-H vibration is considered to reflect the modulated change of the neighboring weak Si-Si bond, the modulation of the weak Si-Si bond should be characterized with the same slow rate of about 10 s^{-1}, which is far from a decay time of nonequilibrium phonons in a Si network.[25] Such a slow response of the vibronic PB signal should be dominated by some electronic process, since the modulation of the electronic PA is also characterized with nearly the same rate. According to my previous work on PL in *a*-Si:H,[26] the PL lifetime, which was evaluated under an experimental condition of geminate-pair recombination, exhibited a relatively long value of 2 ms at 13 K, indicating that excess carriers at tail states can survive longer than a few ms. So the recombination between a photogenerated electron-hole pair trapped at the tail states is considerable as a rate-limiting process in the vibronic modulation.

VI. SUMMARY

The real-time modulation of the Si-H stretching vibration following the modulated excitation can be observed as the photoinduced bleaching band around 2000 cm^{-1} as reported first by Vardeny *et al.*[9] We have considered this vibronic PB band as a result of modulation of the neighboring weak Si-Si bonds following the modulated excitation. Then, when the amount of the weak Si-Si bonds is altered intentionally, some change should be induced in the PB spectrum and a close correlation is expected to exist between the changes in the PB spectrum and dangling-bond density. Based on this idea, we have performed two kinds of studies, the light-soaking and thermal annealing studies, in order to see how the vibronic modulation is affected by breaking or reforming the weak Si-Si bonds. By evaluating quantitatively the spectral change of the PB band combined with the simultaneous change in the ESR spin density, the density of the weak Si-Si bonds or neighboring Si-H bonds, which are precursor sites for the structural flexibility, can be evaluated to be about 5×10^{17} cm^{-3}.

It is noteworthy that the PB spectrum for one specimen, which was prepared at a low substrate temperature and its Si-H stretching vibration was dominated by the 2100 cm^{-1} component, is centered nearby 2000 cm^{-1}, indicating that the vibronic modulation is related selectively with the monohydride bond of Si-H.

Furthermore, since the hydrogen contents contributing to the monohydride Si-H bonds is the order of 10^{21} cm^{-3} in the specimens used here, the density of the Si-H bonds responsible for the structural flexibility is only a very small fraction of them.

ACKNOWLEDGMENTS

The author greatly thanks Dr. G. Ganguly for preparing specimens and Dr. I. Sakata for his kindness when performing ESR measurements.

[1] K. Shimakawa, A. Kolobov, and S. R. Elliot, Adv. Phys. **44**, 475 (1995).
[2] C. S. Hong and H. L. Hwang, Appl. Phys. Lett. **49**, 645 (1986).
[3] R. Darwich, P. R. Cabarrocas, S. Vallon, R. Ossikovski, P. Morin, and K. Zellama, Philos. Mag. B **72**, 363 (1995).
[4] Y. Zhao, D. Zhang, G. Kong, G. Pan, and X. Liao, Phys. Rev. Lett. **74**, 558 (1995).
[5] M. Stutzmann, Philos. Mag. B **56**, 63 (1987).
[6] M. Stutzmann, W. B. Jackson, and C. C. Tsi, Appl. Phys. Lett. **45**, 1075 (1984).
[7] S. Yamasaki and J. Isoya, J. Non-Cryst. Solids **164-166**, 169 (1993).
[8] H. M. Brantz, Phys. Rev. B **59**, 5498 (1999).
[9] Z. Vardeny and M. Olszakier, J. Non-Cryst. Solids **97&98**, 109 (1987).
[10] H. A. Stoddart, Z. Vardeny, and J. Tauc, Phys. Rev. B **38**, 1362 (1988).
[11] I. Hirabayashi, K. Morigaki, and S. Nitta, Jpn. J. Appl. Phys. **19**, L357 (1980).
[12] F. Yonezawa, S. Sakamoto, and M. Hori, J. Non-Cryst. Solids **137&138**, 135 (1991).
[13] A. A. Langford, M. L. Fleet, B. P. Nelson, W. A. Lanford, and N. Maley, Phys. Rev. B **45**, 13 367 (1992).
[14] H. T. Grahn, C. Thomsen, and J. Tauc, Opt. Commun. **58**, 226 (1986).
[15] P. O'Connor and J. Tauc, Phys. Rev. B **25**, 2748 (1982).
[16] Even if dangling bonds are induced by breaking some bond other than a weak Si-Si bond, such as the nearby Si-H bond as suggested by Brantz (Ref. 8), the meaning of N_0 and the procedures for evaluating it as presented in Secs. V A and V B still hold as far as two dangling bonds are formed after breaking the bond followed by their stabilization.
[17] L. Chen, J. Tauc, J. Kocka, and J. Stuchlik, Phys. Rev. B **46**, 2050 (1992).
[18] J. Dauwen and W. Grevendonk, J. Non-Cryst. Solids **114**, 295 (1989).
[19] R. A. Street, Adv. Phys. **30**, 593 (1981).
[20] In my previous work [J. Non-Cryst. Solids **227-230**, 120 (1998)], a preliminary analysis was made on the spectral change of the PB band which was induced by the light soaking, but an argument concerning the defect-quenching effect was not convincing.

[21] J. H. Yoon and C. H. Lee, J. Non-Cryst. Solids **209**, 193 (1997).
[22] S. Oguz, D. A. Anderson, and W. Paul, Phys. Rev. B **22**, 880 (1980).
[23] R. Biswas and Y.-P. Li, Phys. Rev. Lett. **82**, 2512 (1999).
[24] M. Cardona, Phys. Status Solidi B **118**, 463 (1983).
[25] M. van der Voort, G. D. J. Smit, A. V. Akimov, and J. I. Dijkhuis, Physica B **263-264**, 283 (1999).
[26] H. Oheda, Phys. Rev. B **52**, 16 530 (1995).